Theory of vibrationally inelastic electron scattering from oriented molecules

J. W. Davenport,* W. Ho, and J. R. Schrieffer

Department of Physics, University of Pennsylvania, Philadelphia, Pennsylvania 19104

(Received 17 October 1977)

The electron scattering cross sections, both elastic and vibrationally inelastic, have been calculated using the $X\alpha$ multiple-scattering method for H_2, N_2, and CO. The accuracy of the calculational scheme is tested by comparing to data from gas-phase measurements. Good agreement is found between theory and experiment. The formalism is then applied to molecules with fixed orientation by freezing out the rotational motion. The differential inelastic scattering cross sections for vibrational excitation exhibit a variety of angular patterns depending upon the molecule and the energy and direction of the exciting electrons. In all cases which have been calculated, the cross section for vibrational excitation is dominated by negative-ion resonances. The angular distribution patterns reflect the symmetry of these ionic states. These calculations indicate the possibilities of using the characteristics of the inelastic-cross-section patterns as a function of the exciting electrons' energy and direction to study molecules adsorbed on a surface.

I. INTRODUCTION

Dill and Dehmer[1] have shown that the multiple-scattering formalism developed by Johnson and co-workers[2] (for bound states) can be adapted easily to problems involving continuum states. This theoretical technique has been applied successfully to photoionization from both core[3] and valence[4] levels for randomly oriented gas-phase molecules[3,4] as well as molecules with fixed orientation.[4,5] In this paper, we apply this technique to elastic[6] and vibrationally inelastic electron scattering from molecules, another problem involving continuum states.[6]

The motivation for this work is the growth in the study of the bonding configuration of molecules adsorbed on a surface by inelastic low-energy-electron scattering.[7-9] The objective is to illustrate the different angular effects that can be observed in the vibrationally inelastic scattering from a molecule whose orientation has been fixed by a surface, as a function of the identity of the molecule and the energy and direction of the incident electron beam. Our approach to this problem is basically the same as it was to the problem of differential photoionization from a molecule of fixed orientation on a surface.[4,10] We assume that if the adsorbed molecule maintains its molecular identity when adsorbed on a surface, the microscopic properties of the scattering process will be given by properties of the gas-phase molecule. This hypothesis has been thoroughly checked for photoemission from molecularly adsorbed CO.[10] For example, if we were investigating the inelastic scattering from CO adsorbed on a surface, caused by the excitation of the CO vibrational mode, we would first calculate the scattering pattern for an isolated molecule with fixed orientation. The surface would only play a role in fixing the orientation and

modifying the incoming- and outgoing-wave fields, as well as screening the long-range part of the potential. In the case of photoemission, these modifications were treated in a macroscopic calculation.[10,33] In a more refined calculation, other effects due to bonding, such as vibrational frequency shifts and damping effects, can be included, although these are small for weak bonding (see Sec. V).

One of the most dramatic features observed experimentally and theoretically in photoemission from molecules is associated with resonant effects in the continuum.[3,4,10] These resonances occur both for molecules in the gas phase or adsorbed on a surface. Resonant effects are known to dominate electron-scattering cross sections in the 1–10-eV range. Therefore, we will spend considerable time discussing the effects of these resonances on the differential scattering cross section, especially for molecules of fixed orientation. In electron scattering these resonances are negative-ion resonances. The incoming electron is temporarily trapped in a virtual bound state of the molecule. For example, H_2 has a σ_u resonance near 3 eV which can be viewed as the antibonding level of H_2. Similarly in N_2 there is a π_g resonance near 2.3 eV and in CO, a π resonance near 1.7 eV. These are one-electron effects in the sense that they do not involve any electronic excitations of the neutral species. Excitation can occur, however, and result in Feshbach resonances which are generally not as broad as the shape resonances. (For example, in CO there is a Feshbach resonance at 10.04 eV which has a width of approximately 0.04 eV. In contrast, the shape resonance has a width of order 1 eV.) The vibrational-excitation cross sections near the shape resonances are relatively large and have been extensively studied in the gas phase.[11] In both N_2 and CO, losses corresponding to the excitation of vibrational states with quantum

number $n = 1$ up to 8 are observed.[12] Many of these phenomena are expected to be found for electron scattering from adsorbed molecules to the extent that they retain their gas-phase characteristics.

In Sec. II we describe the details of the formalism. The calculated gas-phase cross sections are compared to experimental data in Sec. III. This section illustrates what a major role the negative-ion resonances play in both the magnitude and angular distributions of the scattered electrons. The good agreement between theory and experiment shown in this section is used as justification for the calculations for molecules of fixed orientation shown in Sec. IV. This section illustrates the effects upon the inelastic-scattering pattern by changing the direction and energy of the incident electron beam. Finally, in the concluding Sec. V, we comment about the applicability of these results in inelastic electron scattering from molecules adsorbed on surfaces.

II. FORMALISM

The full Hamiltonian contains electron-electron, electron-nuclear, and internuclear interactions. We write it as

$$H = H_M + T_e + V(\vec{r}, \vec{R}) , \qquad (2.1)$$

where H_M represents the target molecule, T_e the kinetic energy of the scattering electron, and V the interaction potential between the scattering electron and the target molecule. In the multiple-scattering method, this interaction potential is approximated in two ways. First the effects of exchange and correlation are taken into account by a term proportional to the one-third power of the charge density. Then

$$V(\vec{r}, \vec{R}) = V_N(\vec{r}, \vec{R}) + V_H(\vec{r}) + V_{xc}(\vec{r}) , \qquad (2.2)$$

where V_N is the nuclear attraction with $\vec{R}$ representing the nuclear and $\vec{r}$ the electronic coordinates. The static electron-electron interaction or the Hartree term is given by

$$V_H(\vec{r}) = \int \frac{e^2 n(r')}{|\vec{r} - \vec{r}'|} d^3 r' , \qquad (2.3)$$

where n is the electron density and V_{xc} is the exchange-correlation potential which we take to be the usual $X\alpha$ form given by

$$V_{xc}(\vec{r}) = -3\alpha e^2 (3n/8\pi)^{1/3} , \qquad (2.4)$$

where α is a parameter of order 0.7.

The second approximation is that the potential is spherically and volume average to the "muffin-tin" form. That is, nonoverlapping spheres are constructed about each nucleus and an outer sphere placed around the entire molecule. Within the

atomic spheres (region I) and outside the outer sphere (region III) the potential is spherically averaged and in between (region II), it is volume averaged to a constant. The exact procedure has been given by Danese and Connally.[13]

We recall that an exact solution to the scattering problem could be obtained if V_{xc} were replaced by $\Sigma(\vec{r}, \vec{r}')$, the electron self-energy, or the optical potential, and this has been carried out for certain model systems and for a few atoms. The self-energy is nonlocal and energy dependent and not easy to compute except in certain limits. For example, at large distances and low energies, Σ approaches the classical polarization potential[14]

$$\Sigma \rightarrow -\alpha_{pol}/r^4 , \qquad (2.5)$$

where α_{pol} is the polarizability. In the $X\alpha$ approximation,

$$V_{xc} = \tfrac{3}{2} \alpha \Sigma_{HF}^0 , \qquad (2.6)$$

where Σ_{HF}^0 is the Hartree-Fock self-energy of a uniform electron gas of density $n(\vec{r})$ in the limit as $E \rightarrow 0$. For $\alpha = \tfrac{2}{3}$, the Kohn-Sham value, $V_{xc} = \Sigma_{HF}^0$. At high kinetic energies the effects of exchange are cut off. This has been treated by Lee and Beni[15] in the context of extended x-ray absorption fine structure (EXAFS). The same type of cutoff occurs for fixed energy as the density decreases. However, it is known, at least for the electron gas, that these cutoffs are not nearly so rapid as are given by Hartree-Fock. Indeed, in the random-phase approximation (RPA) the self-energy is nearly constant and somewhat larger than the Kohn-Sham value up to $p \sim 2k_F$,[14] where p is the Thomas-Fermi local momentum, and k_F the local Fermi momentum. Consequently, the $X\alpha$ potential is adequate in the interior of the molecule where the density is high. However, in the outer-sphere region, the $X\alpha$ potential should be cut off and matched onto the polarization potential. We have chosen an exponential cutoff because, for example, the Hartree-Fock self-energy goes like

$$\Sigma_{HF} \rightarrow -2\pi e^2 n/p^2 \qquad (2.7)$$

for p/k_F large and n is dropping off exponentially with a decay length of order 2. So we take the potential in region III to be

$$V(\vec{r}, \vec{R}) = -\alpha_{pol}/r^4 + V_0 e^{-2r} , \qquad (2.8)$$

and have chosen V_0 so that V matches the $X\alpha$ potential at the starting point of the radial mesh (which is just inside the outer sphere). The cross sections are not very sensitive to the form of the cutoff. It would be useful to study the effects of higher-order multipoles in describing the long-range part of the potential, since the polarizibility is in general anisotropic.

Finally, the density which determines the potential in the $X\alpha$ method is the total density for the system, target plus incident electron. Ordinarily the ground-state density of the target is a good approximation to the total and this approximation works well for H_2 where the σ_u resonance is fairly broad. For the narrow resonances in N_2 and CO we have found that the density of the scattering electron must be included and we have done this approximately as discussed in Sec. III. This makes sense for narrow resonances because the density due to the scattering electron in the region of the molecule would be expected to be large.

Given the Hamiltonian in Eq. (2.1), let Ψ_M be the target wave functions which are eigenfunctions of H_M. The full transition amplitude between target states M and M' and electron state $\vec{k}$ and $\vec{k}'$ is given by

$$f(\vec{k}M \rightarrow \vec{k}'M') = (-M/2\pi\hbar^2)\langle e^{i\vec{k}'\cdot\vec{r}}\Psi_{M'}|V|\Psi(\vec{r},\vec{R})\rangle , \quad (2.9)$$

where Ψ is an eigenfunction of the full Hamiltonian. In fact, we shall make the adiabatic approximation that

$$\Psi(\vec{r},\vec{R}) = \Psi_M(\vec{R})\Psi_e(\vec{r},\vec{R}) , \quad (2.10)$$

where $\Psi_e(\vec{r},\vec{R})$ is a solution of

$$H_e = T_e + V , \quad (2.11)$$

for fixed $\vec{R}$. Further, we take this solution to have the asymptotic form

$$\Psi_e(\vec{r},\vec{R}) \rightarrow e^{i\vec{k}\cdot\vec{r}} + f_{\vec{k}\vec{k}'}(\vec{R})\, e^{ikr}/r , \quad (2.12)$$

so that f is the elastic-scattering amplitude at fixed $\vec{R}$. Then within the adiabatic approximation and neglecting the difference between the magnitudes k and k' the transition amplitude is given by[16]

$$f(\vec{k}M \rightarrow \vec{k}'M') = \int d^3R\, \Psi_{M'}^*(\vec{R})f_{\vec{k}\vec{k}'}\Psi_M(\vec{R}) . \quad (2.13)$$

The adiabatic approximation is justified on physical grounds because the interaction time (crudely, the time it takes for an electron to traverse the molecule, 10^{-16} sec) is small compared with the vibrational period (10^{-14} sec) or the rotational period (10^{-11} sec). In fact, for the narrow resonances observed in N_2 and CO, the cross sections contain fine structure which has been attributed to nonadiabatic processes since adiabatic theories do not reproduce it. (See Refs. 11 and 17 and Figs. 2 and 6.) However, this fine structure is clearly of secondary importance and we have not treated it.

Since we are interested in vibrational excitations of the target, we take

$$\Psi_M(\vec{R}) = \chi_v(\vec{R}) , \quad (2.14)$$

where χ_v is a vibrational wave function assumed to be that of a harmonic oscillator with vibrational

frequency given by the observed excitation energy. It is natural to expand the scattering amplitude in partial waves

$$f_{\vec{k}\vec{k}'} = \sum_{L,L'} Y_L(\hat{k})f_{LL'}(R)Y_{L'}(\hat{k}') , \quad (2.15)$$

where the Y's are the real spherical harmonics and L is a double index (l, m). Since the Y_L form a complete set, this is general. As shown in the Appendix $f_{LL'}$ (which is proportional to the T matrix) is given by

$$f_{LL'} = \sum_\Lambda -\frac{4\pi}{k}\, i^{l'-l}(1+iK)^{-1}_{L\Lambda}K_{\Lambda L'} , \quad (2.16)$$

where K is a real symmetric matrix, $k^2 = E = $ kinetic energy, and $\Lambda = (\lambda, \mu)$. For spherical potentials

$$K_{L\Lambda} = -\tan\eta_l\delta_{l\lambda}\delta_{m\mu} , \quad (2.17)$$

where η_l is the phase shift. Then

$$f_{LL'} = \frac{4\pi}{k}\, e^{i\eta_l} \sin\eta_l\delta_{ll'}\delta_{mm'} , \quad (2.18)$$

the well-known expression for the scattering amplitude. Since our molecular potentials are not spherically symmetric over all space, the full K matrix must be computed. However, we can use symmetry to block diagonalize K and for linear molecules find partial amplitudes for σ, π, δ, etc. scatterings. Then, the differential cross section for an oriented molecule is given by

$$\frac{d\sigma}{d\Omega} = \left| \sum_{LL'} Y_L(\hat{k})\langle v'|f_{LL'}(R)|v\rangle Y_{L'}(\hat{k}') \right|^2 . \quad (2.19)$$

For the gas phase the amplitude should be transformed to the laboratory frame and matrix elements taken between molecular rotational states. In this paper we wish to compare our calculations with gas-phase data in which rotational excitations were not resolved. Assuming a thermal distribution of initial rotational states and summing over all final rotational states is equivalent to averaging Eq. (2.19) over all orientations of the molecule. The dependence on orientation comes from $\hat{k}$ and $\hat{k}'$, which are defined in the molecular frame. The total gas-phase cross section can be obtained directly by integrating over $\hat{k}'$ and averaging over k to give

$$\sigma = \frac{1}{4\pi} \sum_{LL'} |\langle v'|f_{LL'}|v\rangle|^2 . \quad (2.20)$$

The differential cross section is given in Appendix B and agrees with Eqs. (46) and (47) of Ref. 1.

III. GAS-PHASE CROSS SECTION

In this section we present results for gas-phase molecules using the technique developed in Sec. II.

TABLE I. Experimental parameters used in the calculation.

	Equilibrium spacing[a]	Mean polarizability[b]	Vibrational energy[a]
	(a_0)	(a_0^3)	(meV)
H_2	1.41	5.33	545
N_2	2.08	11.88	293
CO	2.13	13.16	269

[a]Reference 19.
[b]Reference 20.

Our purpose is to show that the $X\alpha$-SW method agrees well enough with the gas-phase data so that it can be used to predict the differential cross sections for the oriented molecules where no angular distribution data exist at the present time. A more complete description of the gas-phase calculation is presented in another paper where simultaneous rotational and vibrational transitions are also discussed for H_2, N_2, and CO.

In Table I we present the experimental parameters used throughout the calculation. The angular independent scattering amplitude $f_{LL'}$ was calculated at five internuclear spacings shown in Table II. For N_2 and CO, the extrema were chosen to correspond approximately to the root-mean-square (rms) displacement of a harmonic oscillator in the $n=4$ state. For H_2, the rms displacement for the $n=4$ state from the equilibrium spacing proved to be too large and the end points were chosen to be somewhat larger than the rms displacement in the $n=1$ state. Therefore, only transitions to the first excited vibrational state were calculated for H_2. The vibrational wave functions were taken to be those of a harmonic oscillator. The scattering amplitude $f_{LL'}$ was fitted to a fourth-order polynomial and (for numerical stability) the vibrational matrix element, e.g., in Eq. (2.20), was integrated numerically using the trapezoidal rule with roughly 150 points. Using Eq. (2.20), we have computed the angle-averaged total cross sections for H_2, N_2, and CO. The result for H_2 is shown in Fig. 1. We found a σ_u resonance which leads to a broad peak in the cross section centered at 4 eV compared

TABLE II. Five internuclear spacings used to calculate the angular independent scattering amplitude $f_{LL'}$.[a]

	Internuclear spacings					Root-mean-square displacement of a harmonic oscillator
H_2	1.11	1.22	1.41	1.56	1.71	0.28 $(n=1)$
N_2	1.88	1.98	2.08	2.18	2.28	0.18 $(n=4)$
CO	1.93	2.03	2.13	2.23	2.33	0.19 $(n=4)$

[a]All distances in atomic units (a_0).
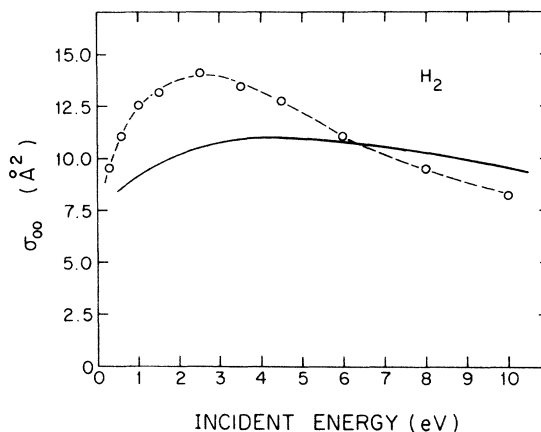
FIG. 1. Elastic scattering cross section for H_2 as a function of the incident energy. The data in dashed curve are from Linder and Schmidt (Ref. 21).

with the experimental value of 3 eV.[21] The absolute cross section agrees to better than 50%. Closer agreement has been obtained with other methods,[22,23] but our results should be adequate in interpreting oriented molecule effects.

We have found that the potentials constructed from the self-consistent ground-state density do not display the π-type resonances found experimentally for N_2 and CO. The reason is that the resonances are narrow and the density of the scattering electron makes a substantial contribution to the self-energy. The potentials for the ground state are too attractive (representing as they do the neutral system). Indeed, there are bound states with π symmetry in both molecules about 2.7 eV below vacuum. If we occupy the N_2 level with one electron and compute a new potential (non-self-consistently), we find a π_g resonance in the scattering cross section at 9 eV. Clearly what is needed is a potential intermediate between the ground state and the negative ion. To produce such a potential, we have extended Slater's transition-state concept and occupied the π level with half an electron.[24] This puts the resonance for N_2 at 3.5 eV (experimental is 2.3 eV) and CO at 4.0 eV (experimental is 1.7 eV). We do not expect this model to produce much better agreement with the data than this although a self-consistent treatment of the resonance state is possible. In fact, if this potential were slightly more attractive, N_2 and CO would have an electron affinity which would be given approximately within the local density theory by the transition-state potential. Therefore, it is entirely reasonable that such a potential should yield an approximate resonance energy.

The total cross sections computed in this way for N_2 and CO are shown in Figs. 2 and 3(a). In the case of N_2, the cross section shows a strong π_g
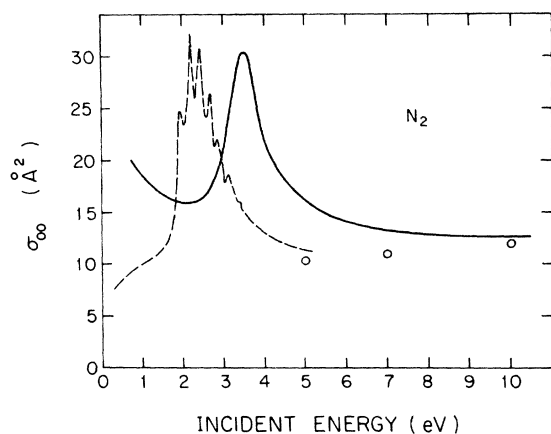
FIG. 2. Elastic scattering cross section for N_2 as a function of the incident energy. Data from Golden (Ref. 25) (dashed curve) and Srivastava, Chutjian and Trajmar (Ref. 26) (O).

resonance and good agreement is obtained with measurements by Golden[25] and by Srivastava *et al.*,[26] except for the fine structure. The rise in calculated cross section below 1 eV is due to the increasing σ_g contribution at low energy, which would diminish if the potential was made more attractive, simultaneously pulling down the resonance. To our knowledge, there is no experimental data for the absolute elastic total cross section of CO, only the relative differential elastic cross section of Ehrhardt *et al.*[27] In Fig. 3(b), comparison is made between the calculation and the data normalized to the calculated peak of 90°. Good agreement is obtained for the shape and the relative intensities of the resonances. Schulz[28] has also given the maximum in the elastic total cross section to be 24.0 $\mathring{A}^2$, which is close to the calculated value of 29.2 $\mathring{A}^2$. All gas-phase measurements indicate that CO and N_2 are very similar, both in the elastic and inelastic scattering cross sections.[27,28] Both show a strong π resonance with the structure in the cross section less pronounced in CO. The width of the resonance is larger for CO than N_2, which has been attributed to the mixture of p and d waves in the resonance, whereas in the π_g resonance of N_2 there is no p wave by symmetry. The experimental fact that the scattering cross sections from N_2 and CO are similar indicates that dipole scattering is not the important process, at least in this energy range.

A comparison of the calculated and measured elastic differential scattering cross sections is a more stringent test of this calculational scheme than is the comparison above of integrated cross sections. We show in Fig. 4(a) the calculated and measured differential elastic cross section for N_2,[26] and the corrresponding curves for CO in Fig.
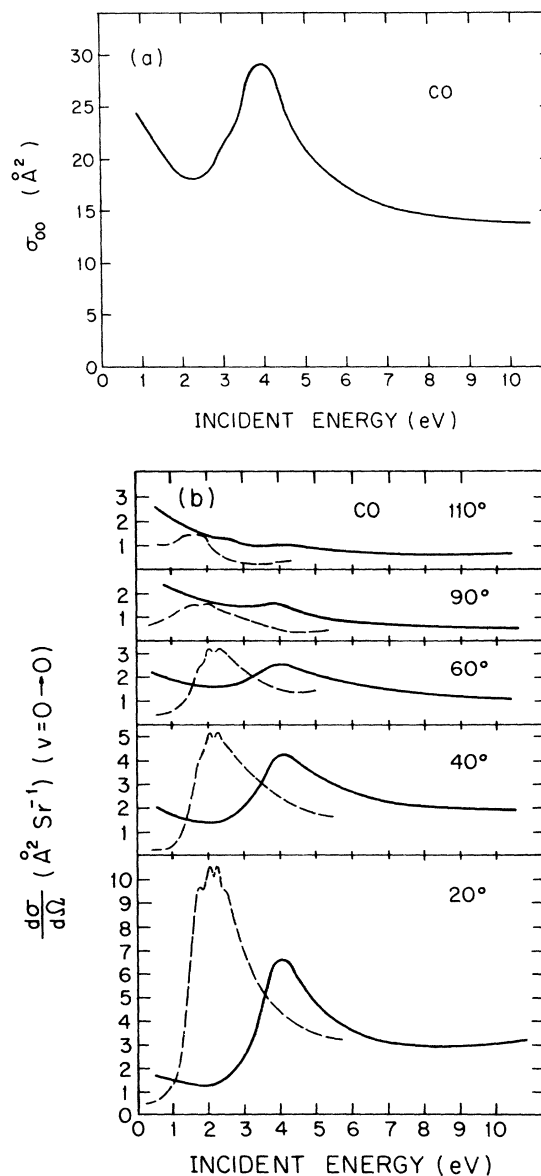
FIG. 3. Elastic scattering cross section from CO as a function of the incident energy. (a) Calculated total scattering cross section. (b) Differential scattering cross section. Data from Ehrhardt *et al.* (Ref. 27) (dashed curves) are normalized to the calculated peak at 90° scattering.

4(b). The experimental data for N_2 are for an incident electron energy of 5 eV. Since our total cross section is shifted to higher energy by approximately 1 eV, the calculated curve is for an incident energy of 6 eV. For CO the measurement is at 2 eV,[27] and the calculation at 4 eV. For N_2 we have the absolute data of Srivastava *et al.*[26] with which to compare. Our calculation is uniformly about 50% higher than the experimental data. Since the data for CO from Ehrhardt *et al.*[27]
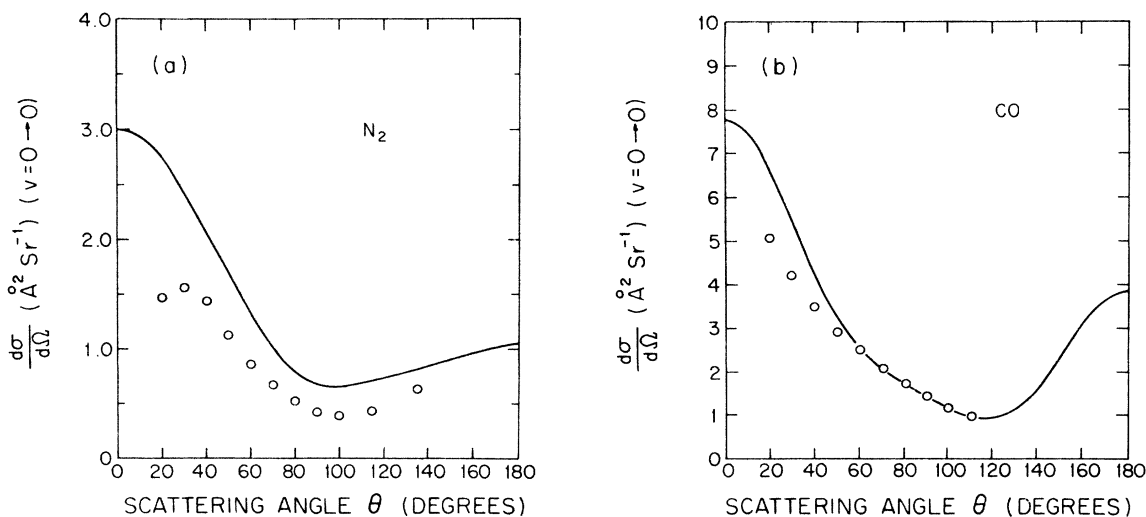
FIG. 4. Differential elastic cross section as a function of the scattering angle for: (a) N_2 at incident energy of 6 eV. The absolute measurement (○) at incident energy of 5 eV is from Srivastava, Chutjian, and Trajmar (Ref. 26). The difference in 1 eV compensates the shift in the peak of the resonance between theory and experiment for the total scattering cross section; and (b) CO at incident energy of 4 eV compared to the data of Ehrhardt et al. (Ref. 27) (○) at 2-eV incident energy, normalized to the calculation at 90°.

is presented in arbitrary units, we have normalized their values to our calculation at 90°. Experimentally the minimum in the CO cross section occurs at a larger scattering angle than it does for N_2. This is also predicted by our calculation. In general, the agreement between theory and experiment for the differential elastic cross section is very good for N_2 and CO.

We now turn to the inelastic cross section. The effect of the negative-ion resonances is much more pronounced in the inelastic cross section than it was in the elastic cross section. Let us first compare the absolute total cross section for exciting a diatomic molecule from the vibrational ground state to the nth state as a function of the energy of the exciting electron. Figure 5 compares our calculated inelastic cross sections with the measurement of Ehrhardt et al.[27] for CO. The measured cross sections for both the 0→1 and 0→2 vibrational transitions are dramatically enhanced at an incident energy corresponding to the negative-ion resonant state. Our calculation, as usual, does not place this resonance at the correct energy, but it does reproduce the magnitude extremely well. Experimentally, the cross section for exciting the first vibrational mode falls by an order of magnitude as the incident electron energy is increased from approximately 1.8 to 3.3 eV. Theoretically, this cross section decreases by a factor of 40 from 3.5 to 10 eV.

Figure 5 also illustrates the enhanced excitation of higher-order vibrational states of the molecule when the excitation energy is near the resonance.

For example, the ratio of the 0→2 to 0→1 cross section at an exciting energy of 3.5 eV is 43%, while it decreases to 7% for a 10-eV incident electron beam. Ehrhardt et al.[27] have shown experimentally that near the resonance the 0→7th mode
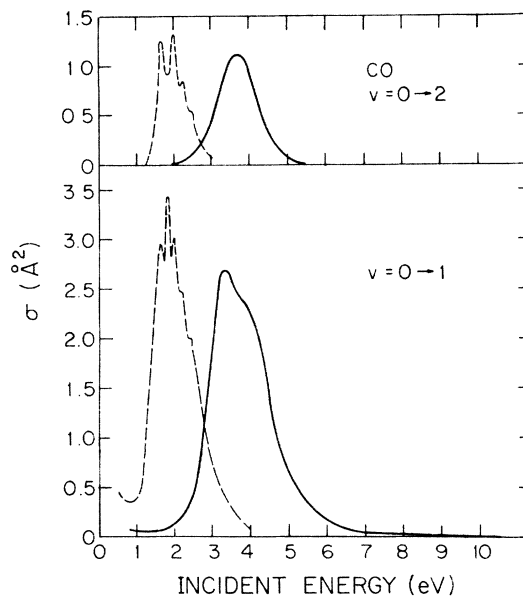
FIG. 5. Total cross section for the 0→1 and 0→2 vibrational transition of CO as a function of the incident energy. The dashed curves are the measurement by Ehrhardt et al. (Ref. 27) with the absolute cross sections obtained from integrating the differential scattering cross sections and normalizing to absolute elastic cross sections.

can be seen in CO with ~6% of the amplitude of the
0→1 transition.

General agreement has also been obtained be-
tween the calculation and the measurement for the
total cross sections of the 0→1 and 0→2 vibration-
al excitation of N_2 and the 0→1 excitation of H_2, as
a function of the incident energy. The resonance
in N_2 is more narrow than CO, both in the theory
and the experiment.[28] The calculated peak of the
resonance is approximately 2-eV higher than the
experiment. However, the relative intensities of
the 0→2 to the 0→1 vibrational excitation are in
good agreement. In H_2, a broad resonance cen-
tered around 4 eV is obtained from the theory and
the experiment.[29,30] The absolute magnitude of the
total cross sections differ by a factor of 2, with the
calculation uniformly larger. However, the gener-
al shape is reproduced very well.

The differential inelastic cross sections for the
0→1 vibrational excitation of N_2 and CO are shown
in Fig. 6. The calculation and measurement are
for an exciting electron energy corresponding to
the maximum in the total cross section (see Fig.
5). This is 1.9 eV for N_2 (Ref. 31) and 1.83 eV for
CO (Ref. 27) experimentally, and 4 eV theoretically
for both molecules. The data are not absolute so
they are normalized at $\theta = 90°$. In N_2 there is a
more pronounced peak in both the experiment and
theory than for CO. This is due to pure d-wave
scattering in the π_g resonance of N_2. For CO the

90° peak is much smaller or nonexisting (experi-
mentally). This is a result of a mixture of p- and
d-wave scattering in the π resonance in CO. For
a pure p-wave scattering, there would be a mini-
mum in the cross section at 90°. Section IV will
illustrate how this p-wave mixture in the CO scat-
tering can produce differential inelastic scattering
cross sections for a molecule of fixed orientation
which are quite different from the equivalent situ-
ation in N_2.

IV. ORIENTED MOLECULES

Section III demonstrated that the theoretical
scheme presented in Sec. II can reproduce reason-
ably well the differential elastic and vibrationally
inelastic electron scattering cross sections for
randomly oriented diatomic molecules. Improved
agreement can be achieved, e.g., in the positions
of the scattering resonances, if a modified multi-
ple-scattering potential is used. To lower the res-
onance energy for e-N_2 elastic scattering, Dill and
Dehmer[6] have used an $X\alpha$ potential with $\alpha = 1$ for
low kinetic energy and obtained improved agree-
ment with experiment. More generally, the
scheme should be generalized to include nonlocal
effects which automatically generate such a vel-
ocity-dependent potential, weakening the exchange-
correlation potential at high energy. In this sec-
tion we apply the theory to diatomic molecules with
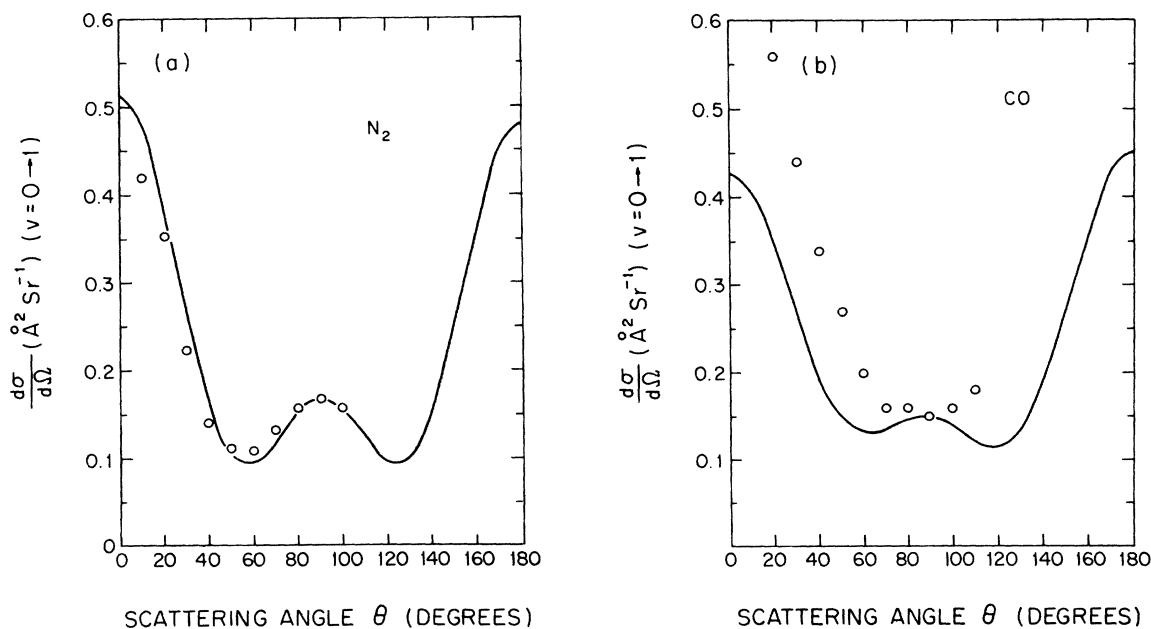
FIG. 6. Differential scattering cross section for the 0→1 vibrational transition as a function of the scattering
angle for: (a) N_2 at 4-eV incident energy. Measurement by Ehrhardt and Willmann (Ref. 31) (○) is at 1.9 eV; and (b)
CO at 4-eV incident energy. Measurement by Ehrhardt *et al.* (Ref. 27) (○) is at 1.83 eV. Both data are normalized
to the calculation at 90°.
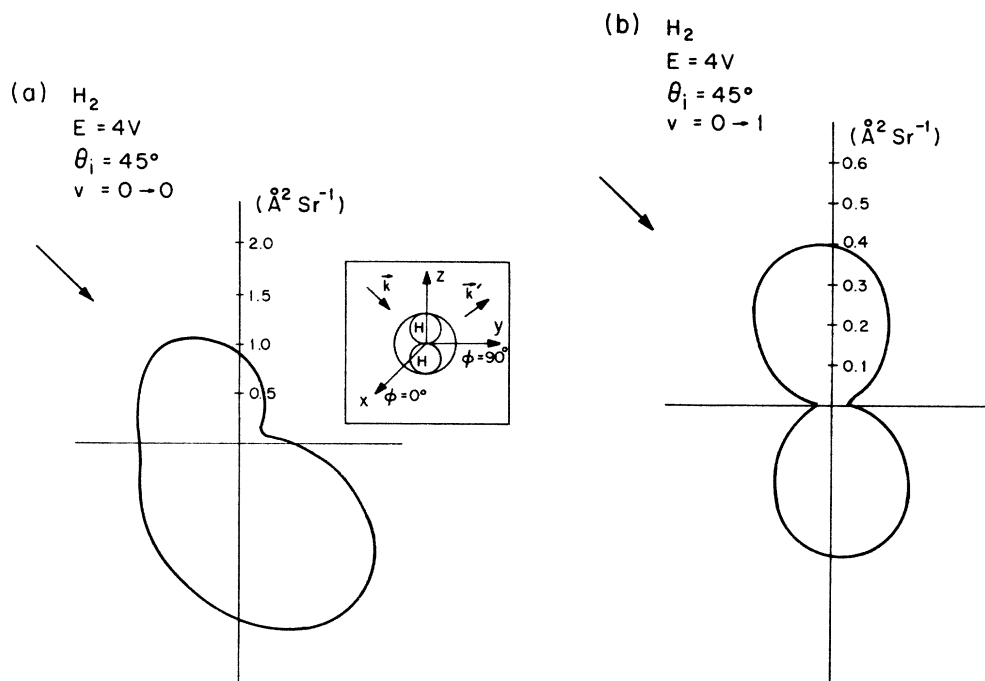
FIG. 7. Polar plots for the angular distribution from oriented H_2 at 45° incidence. (a) Elastic scattering. (b) $0 \rightarrow 1$ vibrational excitation. The incident energy is chosen close to the peak in the total vibrational excitation in the gas phase. Note the difference in the scale.

fixed orientation. The scattering process will still be dominated, as it was in the gas phase, by resonances. When the molecule has a fixed orientation, the negative-ion resonance should have two quite separate effects upon the inelastically scattered angular distribution patterns. First, the probability for forming the negative-ion virtual bound state (resonance) should depend not only upon the incident electron energy, but also upon its direction. This is simply a consequence of the symmetry of the negative-ion state. The second effect is in the angular distribution patterns which again reflect the symmetry of the resonant state. For example, if the resonant state is totally d wave (p wave) as it is in N_2 (H_2), then the angular distribution would look like a d wave (p wave) independent of the angle of incidence of the exciting beam. This angle would only change the amplitude. However, if the resonant inelastic scattering is a mixture of two waves, as it is in CO, we will have angular distribution patterns which change not only in amplitude, but in structure, as the incident direction is changed. This effect results from the angle of incidence dependence of the different partial-wave components in the inelastic cross section.

The first example we present is for oriented H_2. Figure 7 displays the calculated elastic and inelastic differential cross section for an incident

energy of 4 eV. Although the hydrogen molecule is not very interesting as a surface adsorbate, the case is chosen to illustrate the variety of angular distribution patterns that are possible. The resonance in H_2 is distinctly different from the resonances in N_2 and CO. It has σ symmetry, while N_2 and CO resonances have π symmetry. What we intend to illustrate with these molecules is the inherently different angular distribution patterns dictated by the different symmetries.

The scattering geometry for the H_2 molecule is shown in the insert in Fig. 7(a). The elastic scattering pattern shown in Fig. 7(a) is peaked in the forward direction. The pattern does not suggest in any obvious way the σ symmetry of the resonance. This is a result of contribution from both the s and p waves in the elastic scattering cross section. In this case both the σ and π symmetry p waves contribute. However, for inelastic scattering the important quantity is the change in the elastic scattering amplitude with changing internuclear spacing. We find, as did Henry and Chang,[32] that the σ_u channel is dominant for vibrational excitation of H_2, i.e., we have only a p_z wave. This is easily seen in the nearly $\cos^2\theta$ dependence in the angular distribution in Fig. 7(b). Given this single wave contribution to the scattering amplitude we can write the inelastic scattering cross section as

(a) N_2
E = 4 V
θ_i = 45°
v = 0 → 0

(b) N_2
E = 4 V
θ_i = 45°
v = 0 → 1
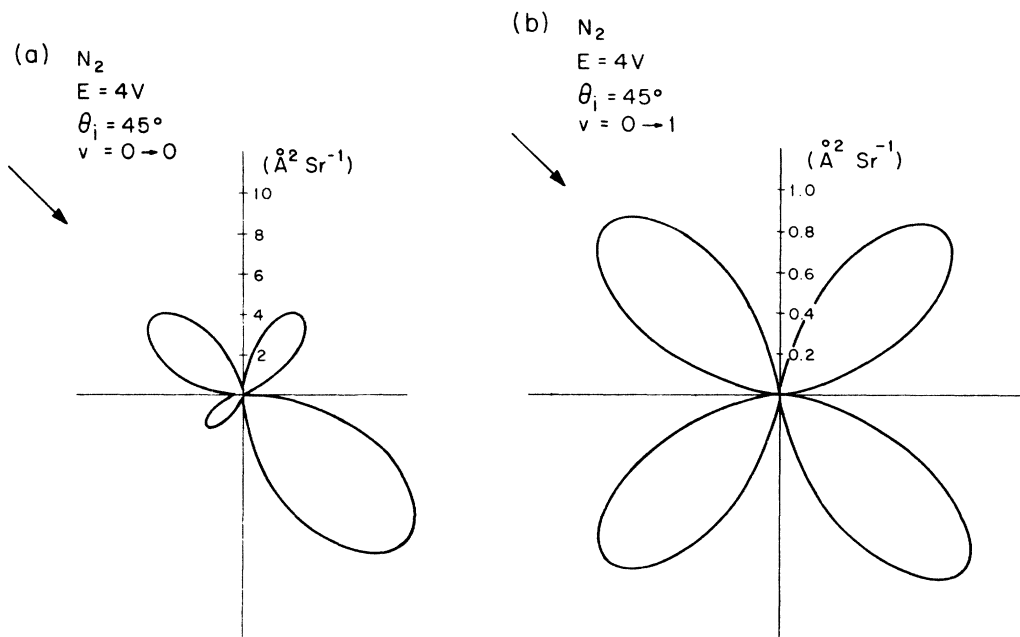
FIG. 8. Polar plots for the angular distribution from oriented N_2 at 45° incidence. (a) Elastic scattering. (b) 0 → 1 vibrational excitation. The incident energy is 4 eV, close to the peak in the total vibrational excitation in the gas phase. Note the difference in the scale.

$$\frac{d\sigma_{01}}{d\Omega}(H_2) = \left(\frac{3}{4\pi}\right)^2 \cos^2\theta_i |\langle 1|f_{p_z}|0\rangle|^2 \cos^2\theta_{out} ,$$

where θ_{out} is the collection angle [Fig. 7(a)], θ_i is the incident angle, and f_{p_z} is the angle-independent scattering amplitude [see Eq. (2.19), $f_{p_z} = f_{11}$].

The inelastic electron scattering pattern from H_2 shown in Fig. 7(b) is now quite simple to understand. The dependence is given solely by the p_z wave and the amplitude varies with the incident electron direction, as the cosine of the angle with respect to the molecular axis. This latter effect is just the probability of forming the p_z component of the negative-ion resonance. Our calculations indicate that even off the resonance one obtains an angular distribution similar to that of Fig. 7(b).

Oriented N_2, which is shown in Fig. 8, is nearly as straightforward as H_2, except that the resonant contribution is in the d waves. The geometry is the same as it was for H_2 in Fig. 7(a). The elastic scattering cross section shows a maximum in the forward direction as it did for H_2, but the d-wave contributions are substantial at right angles to the incident beam. The π_g resonance completely dominates the 0 → 1 inelastic vibrational transition. Due to the symmetry of this π_g state, only the d wave contributes to the scattering and the p wave is excluded. Therefore, to very high accuracy the cross section can be obtained by neglecting all but

the d wave of π symmetry, i.e., the $l = 2$, $m = \pm 1$. This effect is shown by the inelastic scattering pattern in Fig. 8(b). Therefore, we again have a situation where the shape of the angular distribution is independent of the incident direction. The intensity maximum occurs at 45° incidence and vanishes with either on axis or perpendicular to the axis

CO
E = 4 V
θ_i = 45°
v = 0 → 0
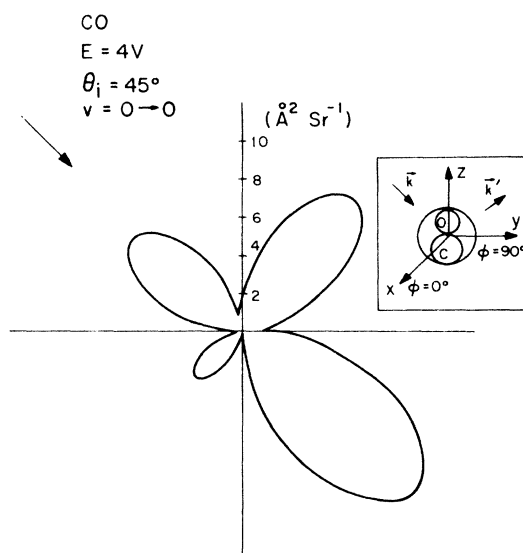
FIG. 9. Polar plot for the elastic scattering angular distribution from oriented CO.

incidence. Off resonance, the overall pattern is preserved, with a decrease in intensity and a skewing of the lobes resulting from other l-wave admixtures.

The final example we present is an oriented CO molecule. The previous two examples illustrated a σ and π resonance with the inelastic scattering completely dominated by a single partial wave. CO again has a π resonance, but due to the lower symmetry than N_2 both the $p\pi$ and $d\pi$ components contribute. The elastic differential scattering cross section is shown in Fig. 9. It looks similar to the elastic scattering pattern for N_2 shown in Fig. 8(a), except that the lobes perpendicular to those along the incident beam direction are larger for CO then for N_2. This reflects the p-d coupling. The difference in the character of the reso-

nances in N_2 and CO is clearly illustrated by the angular distribution of the $0\rightarrow 1$ vibrational transition, shown in Figs. 8(b) and 10(a) for a 45° incident beam. For CO the inelastic cross section is not well approximated by the d-wave or the p-wave contribution alone. The two waves mix and interfere, and one needs to include both to account for the angular distribution. Due to the interference between the two waves, the angular patterns and intensities are strong functions of the direction of incidence. Figures 10(a)-(c) show the angular distribution for the $0\rightarrow 1$ vibrational excitation for three different incident directions. The cross section for incidence along the axis of the molecule is so small [Fig. 10(c)] that it has to be blown up by a factor of 10^3 in Fig. 10(d). This decrease of three orders of magnitude is solely a result of being unable to form the negative-ion resonance with electrons incident parallel to the molecular axis. The p-d mixing allows the incident electron to couple to the resonance when it is incident perpendicular to the axis [Fig. 10(b)], in contrast to N_2. Inspection of the angular pattern in Fig. 10(b) indicates that the dominant term in the inelastic scattering is the outgoing d wave, while the incident direction can only couple to the $p\pi$ resonance. Therefore, this geometry is predominantly p in and d out.

Figure 11 is a semilogarithmic plot of the $0\rightarrow 1$ vibrational-excitation cross section for CO as a function of the energy for two different collection angles. The solid line is for a 50° collection angle which is nearly perpendicular to the incident di-
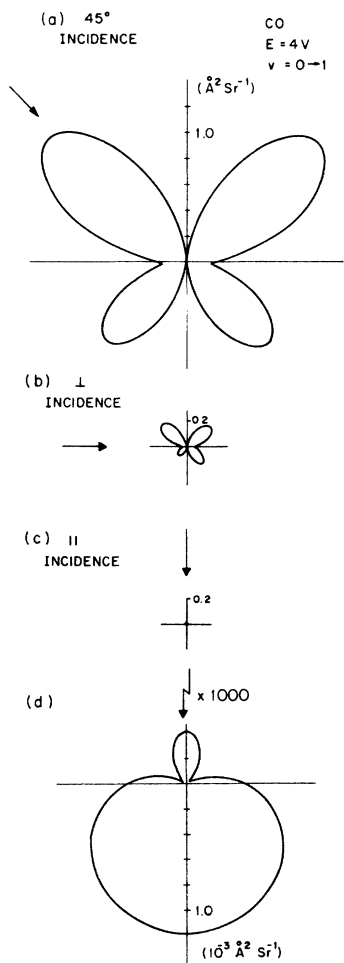
FIG. 10. Polar plots for the $0\rightarrow 1$ vibrational excitation angular distribution from oriented CO. (a) 45° incidence. (b) Perpendicular to the molecular axis incidence. (c) Parallel to the molecular axis incidence. (d) Part (c) blown up 1000 times in scale.
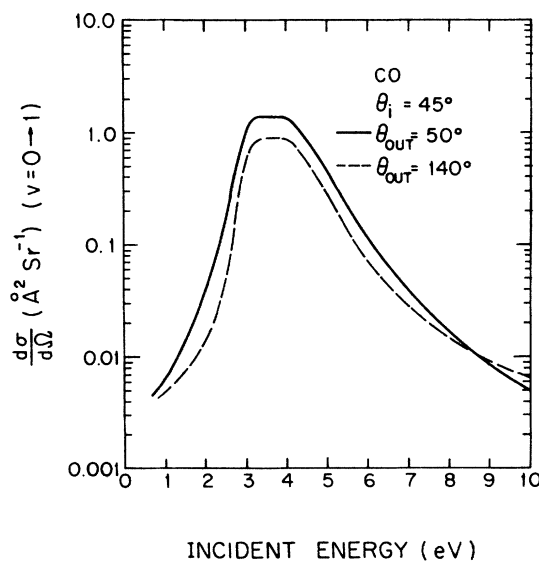
INCIDENT ENERGY (eV)

FIG. 11. Intensity at 50° (solid line) and 140° (dashed line) scattering angles (both at $\phi = 90°$) for CO as a function of the incident energy for 45° incident angle.

rection. The dashed curve is $140°$ collection, which is almost forward scattering. The full width at half-maximum of both curves is approximately 2 eV. At the peak in the resonance, the perpendicular scattering is about 50% larger than the forward scattering. At an incident energy of 10 eV, the forward scattering is about 40% larger than the perpendicular scattering, with both cross sections decreased by nearly a factor of 200.

V. MOLECULES ADSORBED ON SURFACES

Section III compared the calculated elastic and inelastic cross sections for several diatomic molecules with the appropriate gas-phase data. The agreement between theory and experiment was sufficiently good that we predicted the elastic and inelastic scattering cross sections for molecules of fixed orientation in Sec. IV. In this section, we would like to speculate about the implications of the results presented in Sec. IV on inelastic electron scattering from a molecule adsorbed on a surface.[7-9]

The presence of the surface modifies the ideal scattering process presented in Sec. IV in several ways.[34-38] The one which has received the most attention is the reflectivity of the substrate which allows the electrons which have scattered in the forward direction from the molecule to be reflected into the detector. Forward scattering is dominated by the long-range part of the electron-molecule interaction potential which is in turn given by the molecular dipole moment (actually only the change in dipole moment with internuclear spacing is important for vibrational excitation). For this reason, current theories have treated the scattering from an oriented dipole, including the classical images, using first-order perturbation theory. The effect of the image is to cancel the interaction with modes which oscillate parallel to the surface and to quadruple the interaction with perpendicular modes leading to the "selection rule" that only perpendicular modes are observed.[39] In contrast, the short-range interaction can excite modes parallel and perpendicular to the surface with nearly equal intensity.

To compare the relative sizes of the long- and short-range parts, we note that Persson[36] using the dipole model applied to Andersson's experiment (approximately $45°$ in and $45°$ out with a beam half-width of $3°$) has given a vibrational differential cross section of 1 $\mathring{A}^2/sr$. This takes no account of substrate reflectivity which could lower this figure by a factor of 5–10. On the other hand, the short-range mechanism gives cross sections of the same size without any reflections at all (cf. Fig. 10).

To compare with the data we assume the sub-

strate has reflectivity R. Then the elastic current in the specular direction is given by R times the incident current I_0. The inelastic current is given by

$$I_1 = \frac{d\sigma}{d\Omega} \, (\theta_{out}) \, n\Omega I_0 , \qquad (5.1)$$

where n is the number of scatterers per unit surface area. The experiment was for one half a monolayer of CO on Ni(100),[9] with the solid angle

$$\Omega \cong 10^{-2} \text{ sr}. \qquad (5.2)$$

Taking a cross section of 1 $\mathring{A}^2 sr^{-1}$

$$I_1/RI_0 = 7 \times 10^{-4}/R . \qquad (5.3)$$

This is in the same range as the measured ratio (10^{-3}). An important difference is that the dipole scattering gives a ratio which is basically independent of R, while the short-range scattering depends on it. This feature could be checked with many existing spectrometers.

The surface may also modify or even destroy the resonances which are so characteristic of the gas phase. In photoemission, spatially localized shape resonances have been found to be essentially unperturbed for CO adsorbed on nickel. Though similar to the negative-ion resonances discussed here, there is still no guarantee that electron scattering resonances exist for adsorbed molecules. The discussion we have given illustrates that if they exist the inelastic scattering cross section will be as large or larger than the best estimates of the dipolar cross sections. The issue can probably be resolved only by experiment.

From an experimental point of view there are several advantages to observing the short-range scattering. First there are no quasi selection rules, so the complete symmetry of the surface molecule may be observed. For example, Wong and Schulz[40] have shown that for inelastic scattering from gas-phase C_6H_6, it is possible to couple to different symmetry vibrational modes by tuning the incident energy to different resonances. Another major advantage is that the experiment does not have to be performed with the specular beam. This means that one does not have to find the inelastic signal in the tail of the elastic signal, nor does one have to worry about "ghosts" in the electron energy analyzer. Finally, it should be obvious from the variation of the angular distributions in the inelastic scattering presented in Sec. IV that the calculated patterns can be used to determine the bonding geometry of the adsorbed molecules. This can be accomplished by changing the energy and direction of the incident beam as well as the direction of detection. In the case of CO, all the results have been calculated with the inci-

dent beam coming in from the oxygen end of the molecule (see Fig. 9). We have found that the intensities of the angular distributions decrease uniformly if the direction of incidence is from the carbon end of the molecule. For example, for $135°$ incidence, the intensity is decreased to 65% of that for $45°$ incidence, with the overall pattern remaining the same. Therefore, it would be impossible to discriminate between these two bonding configurations from the electron scattering angular distributions. However, by coupling to angular resolved photoemission measurement, the absolute bonding configuration of molecules on surface can in principle be elucidated.

The possibilities seem quite endless given that the negative-ion resonances can be documented experimentally.

ACKNOWLEDGMENTS

APPENDIX A: MULTIPLE-SCATTERING EQUATIONS

The multiple-scattering theory has been treated in detail previously[1] so we merely sketch the results here.

The wave function in the atomic spheres can be written

$$\Psi(\vec{r}_i) = \sum_L A_L^i f_l^i(r_i) Y_L(\hat{r}_i), \tag{A1}$$

where f is the regular solution of the radial Schrödinger equation, and Y_L is a real spherical harmonic. In the outer sphere

$$\Psi(\vec{r}_1) = \sum_L [A_L^1 f_l^1(r_1) + B_L^1 g_l^1(r_1)] Y_L(\hat{r}_1), \tag{A2}$$

which contains both regular and irregular solutions. The wave function in the constant potential region is obtained using Green's theorem and is given by

$$\Psi(\vec{r}) = \sum_{L, j \neq 1} C_L^j n_l(kr_j) Y_L(\hat{r}_j)$$
$$+ \sum_L C_L^1 j_l(kr_1) Y_L(\hat{r}_1), \tag{A3}$$

where j and n are the usual spherical Bessel functions. Matching the functions and their derivatives

at all the sphere boundaries leads to the inhomogeneous equation

$$\sum_{j, L'} G_{LL'}^{ij} C_{L'}^j = \frac{(g_l^1, f_l^1)}{(g_l^1, n_l)} A_L^i \delta_{i1}. \tag{A4}$$

In this equation,

$$(g, f) = g \frac{df}{dr} - f \frac{dg}{dr}, \tag{A5}$$

with the functions and their derivatives evaluated on the sphere boundary. The diagonal parts of G are given by the negative of the cotangent of the sphere phase shifts

$$G_{LL'}^{ii} = \frac{(f_l^i, n_l)}{(f_l^i, j_l)} \delta_{LL'}, \quad i \neq 1, \tag{A6}$$

for the atomic spheres and by

$$G_{LL'}^{11} = \frac{(g_l^1, j_l)}{(g_l^1, n_l)} \delta_{LL'}, \quad i = 1, \tag{A7}$$

for the outer sphere. The off-diagonal parts of G are the structure constants which are the coefficients in the expansion of the free-particle Green's function about two different sites and are given by

$$G_{LL'}^{ij} = \sum_{L''} 4\pi i^{l'' + l - l'} I_R(L', L'', L)$$
$$\times n_{l''}(kR_{ij}) Y_{L''}(\hat{R}_{ij}), \tag{A8}$$

and if i or $j = 1$, then n is to be replaced by j. Here I_R is the real Gaunt integral

$$I_R(L, L', L'') = \int Y_L(\hat{r}) Y_{L'}(\hat{r}) Y_{L''}(\hat{r}) d\Omega. \tag{A9}$$

As discussed elsewhere it is convenient to find solutions of the Schrödinger equation having the form

$$\Psi_L = \sum_{L'} [f_{l'}^1(r_1) \delta_{LL'} + K_{LL'} g_{l'}^1(r_1)] Y_{L'}(\hat{r}_1), \tag{A10}$$

which defines the real symmetric K matrix. Then K is given by

$$K_{LL'} = \frac{(n_l, j_l)}{(g_l^1, n_l)} (G^{-1})_{LL'}^{11} \frac{(g_{l'}^1, f_{l'}^1)}{(g_{l'}^1, n_{l'})} - \frac{(f_l^1, n_l)}{(g_l^1, n_l)} \delta_{LL'}. \tag{A11}$$

To solve the scattering problem we take a linear combination of the Ψ_L and choose the coefficients so that the asymptotic form of the wave function is given by Eq. (2.12). This leads directly to the result for the scattering amplitude given in Eq. (2.16).

APPENDIX B: GAS-PHASE DIFFERENTIAL CROSS SECTIONS

To average the differential cross section over molecular orientations we write Eq. (3.19) as

$$\frac{d\sigma}{d\Omega} = \sum_{\substack{LL' \\ \Lambda\Lambda'}} Y_L(\hat{k}) Y_{L'}(\hat{k}) \bar{f}^*_{L\Lambda} \bar{f}_{L'\Lambda'} Y_\Lambda(\hat{k}') Y_{\Lambda'}(\hat{k}') , \qquad (B1)$$

where $\bar{f}$ denotes the vibrational matrix element. The Y's can be combined using the Gaunt integral (Eq. A9),

$$\frac{d\sigma}{d\Lambda} = \sum_{\substack{LL'L'' \\ \Lambda\Lambda'\Lambda''}} I_R(LL'L'') I_R(\Lambda\Lambda'\Lambda'') \bar{f}^*_{L\Lambda} \bar{f}_{L'\Lambda'}$$
$$\times Y_{L''}(\hat{k}) Y_{\Lambda''}(\hat{k}') . \qquad (B2)$$

Next rotate the Y's into the lab frame using[18]

$$Y_{lm} = \sum_\mu Y_{l\mu} D^l_{\mu m}(\alpha\beta\gamma) , \qquad (B3)$$

where α, β, and γ are the Euler angles which specify the molecular orientation. Then, using the orthogonality of the D's and the addition theorem for spherical harmonics we obtain

$$\frac{d\sigma}{d\Omega} = \sum_{l''} A_{l''} P_{l''}(\cos\theta) , \qquad (B4)$$

where

$$A_{l''} = \frac{1}{4\pi} \sum_{\substack{LL' \\ \Lambda\Lambda'}} I_R(LL'L'') I_R(\Lambda\Lambda'\Lambda'') \bar{f}^*_{L\Lambda} \bar{f}_{L'\Lambda'} , \qquad (B5)$$

and $P(x)$ is the usual Legendre polynomial.

*Present address: Institute of Theoretical Physics, Fack, S-402 20 Göteborg, Sweden.

[1]D. Dill and J. L. Dehmer, J. Chem. Phys. <u>61</u>, 692 (1974).

[2]K. H. Johnson, Adv. Quantum Chem. <u>7</u>, 143 (1973).

[3]J. L. Dehmer and D. Dill, Phys. Rev. Lett. <u>35</u>, 213 (1975); J. Chem. Phys. <u>65</u>, 5327 (1976).

[4]J. W. Davenport, Phys. Rev. Lett. <u>36</u>, 945 (1976).

[5]S. Wallace, D. Dill, and J. L. Dehmer (unpublished).

[6]D. Dill and J. L. Dehmer, Phys. Rev. A <u>16</u>, 1423 (1977).

[7]The first high-resolution experiment on low-energy electron scattering from surface adsorbates was reported by F. M. Propst and T. C. Piper, J. Vac. Sci. Technol. <u>4</u>, 53 (1967).

[8]H. Ibach, Surf. Sci. <u>66</u>, 56 (1977); H. Froitzheim, H. Ibach, and S. Lehwald, Phys. Rev. B <u>14</u>, 1362 (1976).

[9]S. Andersson, Solid State Commun. <u>20</u>, 229 (1976); <u>21</u>, 75 (1977).

[10]E. W. Plummer and T. Gustafsson, Science <u>199</u>, 165 (1977).

[11]See review article by G. J. Schulz, Rev. Mod. Phys. <u>45</u>, 423 (1973).

[12]M. J. W. Boness and G. J. Schulz, Phys. Rev. A <u>8</u>, 2883 (1973).

[13]J. B. Danese and J. W. D. Connolly, J. Chem. Phys. <u>61</u>, 3063 (1974).

[14]L. Hedin and S. Lundqvist, Solid State Phys. <u>23</u>, 1 (1969).

[15]P. A. Lee and G. Beni, Phys. Rev. B <u>15</u>, 2862 (1977).

[16]D. M. Chase, Phys. Rev. <u>104</u>, 838 (1956).

[17]A. Temkin, Comments At. Mol. Phys. <u>5</u>, 129 (1976).

[18]M. E. Rose, *Elementary Theory of Angular Momentum* (Wiley, New York, 1957).

[19]G. Herzberg, *Molecular Spectra and Molecular Structure, Spectra of Diatomic Molecules* (D. Van Nostrand, New York, 1950), Vol. I.

[20]J. O. Hirschfelder, C. F. Curtiss, and R. B. Bird, *Molecular Theory of Gases and Liquids* (Wiley, New York, 1954).

[21]F. Linder and H. Schmidt, Z. Naturforsch. A <u>26</u>, 1603 (1971).

[22]S. Hara, J. Phys. Soc. Jpn. <u>27</u>, 1009 (1969).

[23]R. J. W. Henry and N. F. Lane, Phys. Rev. <u>183</u>, 221 (1969).

[24]J. C. Slater, Adv. Quantum Chem. <u>6</u>, 1 (1972).

[25]D. E. Golden, Phys. Rev. Lett. <u>17</u>, 847 (1966).

[26]S. K. Srivastava, H. Chutjian, and S. Trajmar, J. Chem. Phys. <u>64</u>, 1340 (1976).

[27]H. Ehrhardt, L. Langhans, F. Linder, and H. S. Taylor, Phys. Rev. <u>173</u>, 222 (1968).

[28]G. J. Schulz, Phys. Rev. <u>135</u>, A988 (1964).

[29]F. Linder and H. Schmidt, Z. Naturforsch. A <u>26</u>, 1603 (1971).

[30]A. G. Englehardt and A. V. Phelps, Phys. Rev. <u>131</u>, 2115 (1963).

[31]H. Ehrhardt and K. Willmann, Z. Phys. <u>204</u>, 462 (1967).

[32]R. J. W. Henry and E. S. Chang, Phys. Rev. A <u>5</u>, 276 (1972).

[33]S. P. Weeks and E. W. Plummer, Solid State Commun. <u>21</u>, 695 (1977).

[34]E. Evans and D. L. Mills, Phys. Rev. B <u>5</u>, 4126 (1972).

[35]D. M. Newns, Phys. Lett. <u>60A</u>, 461 (1977).

[36]B. N. J. Persson, Solid State Commun. <u>24</u>, 573 (1977).

[37]F. Delanaye, A. Lucas, and G. D. Mahan (unpublished).

[38]D. Šokčević, Z. Lenac, R. Brako, and M. Šunjić Z. Phys. B <u>28</u>, 273 (1977).

[38]These selection rules are weakly broken if the molecule does not lie precisely in the image plane.

[40]S. F. Wong, and G. J. Schulz, Phys. Rev. Lett. <u>35</u>, 1429 (1975).